Pathogen threat proximity shapes host extracellular vesicle production in pre-infection response

Klaudia Kołodziejska[1], Agata Szczepańska[1], Nathalie Pujol[2], Wojciech Pokrzywa[3], Michał Turek[1]

Affiliations:

[1]*Laboratory of Animal Molecular Physiology, Institute of Biochemistry and Biophysics, Polish Academy of Sciences, Warsaw, Poland*

[2]*Aix Marseille Univ, INSERM, CNRS, CIML, Turing Centre for Living Systems, 163 Avenue de Luminy, case 906, 13009 Marseille, France*

[3]*Laboratory of Protein Metabolism, International Institute of Molecular and Cell Biology in Warsaw, Poland*

Correspondence should be directed to:

MT: m.turek@ibb.waw.pl

Abstract

Extracellular vesicles (EVs) play a crucial role in immune responses, yet it remains unclear whether pathogen metabolites alone can stimulate EV production prior to infection. Using *Caenorhabditis elegans*, we investigate this question through the lens of exophers – large, evolutionarily conserved EVs known to enhance proteostasis, extend lifespan, and improve reproductive fitness. Our study uncovers distinct regulatory mechanisms driving EV production in response to pathogen-derived volatile and non-volatile metabolites, providing insights into host-pathogen signaling before physical interaction. We reveal a sophisticated network that adjusts EV production based on pathogen proximity: non-volatile metabolites, signaling an immediate threat, activate immune-dependent EV pathways, while volatile metabolites, forewarning potential danger, initiate immunity-independent exopher production. Both responses rely on sensory neurons, with ASK, ADL, and AWC neurons playing central roles in each, and additional input from ASI, AWB, and ASH neurons specifically enhancing non-volatile-induced EV production. Multiple GPCRs, including SRI-19, SRI-36, SRI-39, and SRR-6, are crucial for the non-volatile response, with signal integration mediated by the AIB interneuron and NPR-9 receptor in both responses. Notably, volatile-induced exopher production enhances offspring survival against pathogens but compromises maternal survival. Thus, our study shows that *C. elegans* distinguishes pathogen proximity through metabolite types, activating EV-dependent physiological responses tailored to either immediate or anticipated threats to optimize survival across generations.

Keywords

C. elegans, extracellular vesicles, exophers, pathogens, immune response, olfactory neurons, GPCRs

Introduction

Extracellular vesicles (EVs), including exosomes and microvesicles, are pivotal in the host immune response by mediating intercellular communication and regulating immune functions. Released by various cell types, EVs carry a diverse array of bioactive molecules such as antigens, signalling molecules, and genetic material, thus influencing immune cell behaviour and activity[1,2]. Pathogen-derived EVs often contain pathogen-associated molecular patterns (PAMPs) that can activate immune responses[3], while host-derived EVs help modulate inflammation and immune activation, maintaining homeostasis and enhancing defence mechanisms against pathogens[4]. These roles for EVs have been well-documented during active infection, where pathogens are already invading the host. However, pathogens release both volatile and non-volatile metabolites, which can alert and prepare the host to their exposure[5,6]. Whether such metabolites can modulate EV production prior to infection is not known.

The nematode *Caenorhabditis elegans* is a widely used model for studying host-pathogen interactions, particularly valuable for examining its responses to clinically significant human pathogens such as *Pseudomonas aeruginosa*, *Serratia marcescens*, and *Staphylococcus aureus*[7]. This organism offers several advantages due to its simplicity, genetic tractability, and well-characterized immune responses. *C. elegans* relies solely on innate immune pathways, making it an ideal organism for dissecting fundamental aspects of innate immunity without the confounding influence of an adaptive immune system[8]. Additionally, its transparent body allows real-time observation of infection processes, and its short lifespan and large brood size enable high-throughput genetic and pharmacological screens[9]. The evolutionary conservation of many immune pathways between *C. elegans* and higher organisms further enhances its relevance for studying host-pathogen interactions[10,11].

C. elegans has emerged as well as a valuable model for studying EV production. Due to its transparent body and well-characterized genetics, *C. elegans* allows to track EV production in

real-time and investigate the regulatory pathways involved[12]. One of the examples of evolutionarily conserved class of particularly large EVs that is investigated in worms are exophers. Exophers have been shown to be involved in waste removal and material exchange between tissues, with key functions in cellular stress responses, tissue maintenance, and reproduction[13–18]. Previous studies have demonstrated that exophers help protect neuronal activity in *C. elegans* by expelling toxic cellular debris[13], a process also observed in mammals, where mouse cardiomyocytes release exophers to discard defective mitochondria, maintaining metabolic balance and preventing inflammation[19]. In addition to waste disposal, exophers have been shown to facilitate inter-tissue transport to facilitate reproductive fitness[14], a process that can be regulated by social signalling derived from other animals within the population[18].

In this context, we aim to investigate whether EV production in a host organism can be modulated by the mere presence of pathogens in the environment. Importantly, we focus on the response to pathogen metabolites, allowing us to decouple this regulation from direct infection-related responses. Using exophers released by *C. elegans* body wall muscles as a model, we seek to explore the molecular mechanisms underlying pathogen metabolites-induced EV dynamics.

Our study uncovers a complex regulatory network governing exopher production in *C. elegans*, shaped by the type of interaction with pathogens. Pathogen infection or exposure to their metabolites increases exopher production. However, the molecular mechanisms regulating volatile- and non-volatile metabolite-dependent increases in EV production are distinctly controlled at immune, sensory, and neuronal levels. Our research demonstrates that worms can differentiate the proximity of a pathogen threat based on the type of metabolites they detect. Non-volatile metabolites, typically sensed at close range, signal the pathogen's immediate presence, whereas volatile metabolites, detected from a greater distance, indicate a nearby pathogen that may pose a lower threat. This ability to distinguish between signals triggers a

context-specific physiological response, which may or may not involve immune activation, depending on the nature of the detected metabolites. These findings provide new insights into the physiological mechanisms of EV production in *C. elegans* and suggest that similar mechanisms may be conserved across species.

Results

Infection with pathogens induces exopher production in hermaphrodite muscles

To verify if pathogen infection influence production of extracellular vesicles in *C. elegans*, we exposed worms at adulthood day 1 to live *Pseudomonas aeruginosa* PA14 or *Serratia marcescens* Db10 bacteria for 3 hours. Next, we moved them back to plates seeded with a non-pathogenic *Escherichia coli* OP50 bacteria and 24 hour later we examined the number of exophers released by body wall muscles (BWMs) in a similar way as described before[20] (**Fig. 1a**). Our results show that worms exposed to both types of pathogenic bacteria produce significantly more exophers than worms that were kept on *E. coli* OP50 bacteria throughout the whole experiment (**Fig. 1b**).

Given that extracellular vesicles in other organisms are often part of the immune response[1,21], we next examined whether basal production of exophers as well as increased exopher production upon exposure to pathogenic bacteria depends on specific immune pathways. We tested various mutants deficient in key nematode immune response pathways[22,23], including the insulin pathway (*akt-1*, *daf-16*)[24], TGFβ pathway (*dbl-1*)[25], p38 MAPK pathway (*tir-1*, *pmk-1*)[26,27], and Intracellular Pathogen Response (IPR) pathway (*cul-6*)[28,29] (**Fig. 1c**). In all tested immune response pathways, we observed altered levels of exophergenesis, either decreased or increased, compared to wild-type worms. This was observed under standard growing conditions on non-pathogenic *E. coli* bacteria after knocking out at least one component of each pathway (**Fig. 1d**). However, when immune response mutants were exposed to pathogens, there was a consistent increase in exopher production across all tested mutants, as observed in wild-type

worms (**Fig. 1e-g**). The exception was the *cul-6* mutant with a compromised IPR pathway, which showed a smaller increase in exopher production upon exposure to *P. aeruginosa* and a decrease in exopher production upon exposure to *S. marcescens* when compared to the wild-type control (**Fig. 1h**). Therefore, the pathogen-induced EV modulation does not rely on canonical immune response pathways.

Because it was shown previously that exopher production depends on the presence of embryos in the uterus[14,30], we have tested whether exposing worms to pathogens causes increased eggs retention which in turns could be responsible for increased exopher production. Our results show that while we could observe increased eggs retention for worms exposed to *S. marcescens* Db10, there was no increase for worms exposed to *P. aeruginosa* PA14 (**Fig. 1i**). This indicates that the *P. aeruginosa*-dependent increase in exopher production operates independently of the previously described embryo-maternal signalling, suggesting the involvement of a novel regulatory pathway. It is possible that *S. marcescens*-mediated EV modulation also occurs via this pathway, but disentangling it from the embryo-maternal effect is more challenging. Therefore, we have focused our investigation exclusively on *P. aeruginosa* to uncover the mechanisms underlying pathogen-induced exopher production.

Pathogen non-volatile and volatile metabolites trigger exopher production

Recent reports indicate that *C. elegans* can detect pathogen volatile metabolites, which influence their physiology in a cell non-autonomous manner[31,32]. Given that, we investigated whether exposure to pathogen odours alone would be sufficient to induce exopher production in muscle cells. To test this, we covered NGM plate seeded with OP50 and containing age-synchronized L4-stage worms with another plate containing *P. aeruginosa* and sealed both plates together with parafilm. Worms were incubated in this setup for 48 hours until they reached adulthood day 2, after which exophers were counted (**Fig. 2a**). Our results demonstrate

that exposure to *P. aeruginosa* volatile metabolites indeed induces exopher production (**Fig. 2b**) as well as causes embryo accumulation *in utero* (**Fig. 2c**).

Previous studies have shown that exposing *C. elegans* to *P. aeruginosa* metabolites leads to a robust immune response[33]. Therefore, we aimed to determine whether the increased production of EVs in response to pathogens requires direct infection or if contact with bacterial metabolites is sufficient (**Fig. 2d**). As shown in **Fig. 2e**, direct infection with *P. aeruginosa* is not necessary; worms grown on plates with *P. aeruginosa* supernatant also produced more exophers. Notably, this increase in exopher production do not depend on increased egg retention in the worm's uterus (**Fig. 2f**).

Next, we investigated whether the increased EVs production in our new experimental setups is influenced by innate immunity signalling pathways. Our results indicate that none of the tested pathways—including insulin, TGFβ, p38 MAPK, and IPR—significantly contribute to the volatile metabolite-dependent increase in EV production (**Fig. 3a and c**). However, there is a notable discrepancy in the role of these pathways when considering the non-volatile metabolite-dependent increase in EV production. Specifically, while the insulin pathway does not appear to be involved, the TGFβ, p38 MAPK, and IPR pathways are essential for the supernatant-dependent increase in exopher production (**Fig. 3b and c**). These results suggest that *C. elegans* relies on distinct immune signalling mechanisms for EV production, activating TGFβ, p38 MAPK, and IPR pathways in response to direct contact with bacterial metabolites, while bypassing these pathways entirely for airborne signals.

Multiple types of sensory neurons regulate exopher production in response to pathogen

Olfactory neurons in *C. elegans* detect numerous environmental signals that influence various aspects of the worm's life, including behaviour, physiology, and reproduction[34]. Additionally, our recent findings have shown that olfactory neurons regulate pheromone-dependent increases in EV production[18]. To identify the sensory neurons responsible for regulating the pathogen

supernatant-dependent and volatile metabolite-dependent increases in EV production, we utilized nematodes with genetic ablations of sensory neurons known to mediate pathogen recognition[35–37]. By systematically analysing the effects of these ablations, we discovered that the removal of either ADL, ASK, or AWC neurons completely abolishes both supernatant-dependent and volatile metabolite-dependent upregulation of exopher production (**Fig. 4a-c**). Conversely, the removal of AQR/PQR/URX previously shown to be responsible for exophergenesis regulation[18] has no effect in either assay (**Fig. 4a-c**). Interestingly, we observed discrepancies among ASI, ASH, and AWB neurons. While ASI, ASH, and AWB neurons are crucial for the supernatant-induced increase they do not play a role in volatile metabolite-dependent increase in EV production (**Fig. 4a-c**). These findings show that multiple types of sensory neurons regulate exopher production in response to pathogen metabolites in a context-dependent manner, with ADL, ASK, and AWC neurons playing pivotal roles.

AIB interneuron and AIB-specific NPR-9 receptor integrate sensory response to mediate exopher production

To understand the neuronal circuit mediating pathogen-induced exopher production, we utilized the available *C. elegans* connectome to search for an interneuron downstream of all sensory neurons involved in this response[38]. This search pinpointed the AIB interneuron, which has previously been implicated in regulating *C. elegans* immunity[39]. According to the same study, the AIB-specific neuropeptide receptor NPR-9 mediates this immune response[39]. Consequently, we investigated the involvement of the AIB interneuron and the NPR-9 receptor in the regulation of exopher production. Our data show that the genetic ablation of the AIB interneuron does not alter exopher production under standard growing conditions, whereas the removal of the NPR-9 receptor leads to a decrease in exopher production (**Fig. 5a**). Additionally, upon exposing worms to *P. aeruginosa* metabolites, we found that the removal of AIB neuron or NPR-9 receptor abolishes the increased exophergenesis induced by pathogen

volatile metabolites (**Fig. 5b and e**) and supernatant (**Fig. 5d and e**). These results suggest that the AIB interneuron and NPR-9 receptor are essential for mediating exopher production in response to pathogen signals

Multiple G-protein coupled receptors control pathogen-induced exopher production

G-protein coupled receptors (GPCRs) are essential mediators that enable cells to interact with their environment by transmitting signals. In both vertebrates and in invertebrates, GPCRs play a key role in coordinating immune responses[40,41]. In order to pinpoint the receptor(s) responsible for binding pathogen-released molecule(s) that modulate exophergenesis, we analysed published transcriptomics data from worms exposed to *P. aeruginosa* PA14 compared to worms grown on *E. coli* OP50[42]. Among the most significantly upregulated GPCRs were *sri-36* and *sri-39*, with fold changes of 480 and 79.5, respectively. According to a study by Vidal et al.[43], these GPCRs are expressed in ASK and ASI cells, which we have shown to play an important role in exopher upregulation (**Fig. 3a-b**). Additionally, our prior RNA sequencing, which identified the GPCR *str-173* as a regulator of socially mediated exopher production, also highlighted *sri-36* and *sri-39* as top candidates, further supporting their potential as strong candidates for validation[44]. To investigate the roles of *sri-36* and *sri-39* in exopher regulation, we employed CRISPR/Cas9 technology to generate a mutant with a deletion encompassing both receptor-encoding genes, as they are located only 1.9 kb apart, with one gene situated between them (**Supplementary Fig. 1**).

Moreover, to identify receptors that regulate exophergenesis and may play a role in stimulating exopher production (potentially through pathogen metabolites), we conducted RNA sequencing on age-synchronized wild-type worms that exhibited either many (more than 20) or few (fewer than 2) exophers on adulthood day 2. A similar strategy, utilizing gene expression heterogeneity within isogenic populations, was recently employed to study the processes that generate lifespan variation[45]. The results of this RNA sequencing show that worms producing many

exophers differ significantly at the transcriptomic level from worms producing few exophers (**Fig. 6a**). Specifically, 609 genes were upregulated and 665 genes were downregulated (p adj < 0.05; -1> log2 fold change > 1) (**Fig. 6b and Supplementary Data 1**). Among the statistically significant GO terms, "cilium assembly" was upregulated in worms producing many exophers (**Fig. 6c**). This finding aligns with our data showing that ciliated neurons are crucial for regulating exophergenesis in muscles (as it was previously shown in Szczepańska, Olek et al.[44]). Notably, three GPCRs—STR-173, SRR-6, and SRI-19—were significantly altered in animals producing varying numbers of exophers (**Fig. 6d**). Importantly, we had previously identified STR-173 as a GPCR regulating exophergenesis via the male pheromone ascr#10, validating our approach[18]. Therefore, we decided to create CRISPR/Cas9-mediated mutants for the *srr-6* and *sri-19* genes encoding GPCRs as well (**Supplementary Fig. 1**).

Among the four GPCRs studied, the removal of each receptor significantly suppressed *P. aeruginosa*-induced exopher production in response to bacterial supernatant (**Fig. 7c, g, k**), but not to volatile metabolites (**Fig. 7b, f, j**). Notably, the basal level of exophergenesis in GPCR mutant worms under standard conditions remained unchanged (**Fig. 7a, e, i**). These findings collectively indicate that these receptors are critical for pathogen-induced exopher production, but not under non-stressed conditions.

The wrmScarlet CRISPR/Cas9-mediated transcriptional knock-in of the *sri-19* gene revealed its specific expression in ADL neurons (**Fig. 7d**). Furthermore, transcriptional reporters using fluorescent proteins for the *sri-36* and *sri-39* genes indicated expression in anterior ciliated neurons (**Fig. 7h**), which, based on available literature[43], correspond to ASI and ASK neurons. This observation is consistent with our data, underscoring the critical role of ADL, ASK, and ASI neurons in pathogen-induced exopher production and establishing its molecular mechanism. Additionally, the expression of the *srr-6* receptor in neurons of the retrovesicular ganglion (RVG), alimentary tract, and excretory system (**Fig. 7l**), as well as the expression of

sri-36 and *sri-39* in the alimentary tract (**Fig. 7h**), suggest that one or more of these tissues may also play a role in regulating exopher production in muscles.

Offspring of animals that produce more exophers after exposure to pathogen volatile metabolites have a higher survival rate post-infection, at the cost of the mother's survival

Building on our findings, which demonstrated an increase in exopher production in the presence of pathogen volatile metabolites, we aimed to investigate the underlying reasons for the release of these extracellular vesicles when worms detect the pathogen in their environment. In *C. elegans* the tissues most frequently involved in host-pathogen defence are those exposed to the environment: the epidermis and the intestine[22,23]. Therefore, it is unlikely that muscle-derived exophers serve as carriers for immune pathway effectors, such as C-type lectins or antimicrobial peptides, between tissues to enhance the immune response. To further explore this, we tested whether worms that produce more exophers due to exposure to *P. aeruginosa* volatile metabolites could survive *P. aeruginosa* infection for a longer period (**Fig. 8a**). Interestingly, we observed that these worms exhibited reduced survival during bacterial infection, which inversely correlates with exopher production (**Fig. 8b**). This result was further correlated by the fact that worms with ablated ASK neurons, that produce fewer exophers than wild type worms (**Fig. 4a-b**), survive *P. aeruginosa* infection longer than wild types (**Fig. 8b**). This also aligns with the fact that worms with the knockdown of the RME-2 receptor, which produce very few exophers[14], also survive *P. aeruginosa* infection longer than wild-type worms (**Fig. 8c**). Thus, it appears that worms producing many exophers after pre-exposure to pathogen volatile metabolites exhibit worse survival during subsequent infection. Additionally, *sri-19* mutants, which do not show increased exopher production upon contact with *P. aeruginosa* non-volatile metabolites, survived significantly longer during infection (**Fig. 8c**) which demonstrates that on mechanistic level survival is interconnected with the regulatory elements for EV production.

Given that muscle exophers have been shown to improve animal reproduction and boost offspring development, we hypothesized that worms producing more exophers in response to pathogen volatile metabolites may have progeny better equipped to survive pathogen exposure during their lifetime. To test this hypothesis, we exposed hermaphrodite mothers (P0 generation) to the volatile metabolites of *P. aeruginosa* from the L4 stage until adulthood day 2. After 48 hours of exposure, we isolated the offspring (F1 generation) and cultured them on plates seeded with *E. coli* until they reached the L4 stage. Subsequently, we transferred these animals to plates seeded with *P. aeruginosa* and monitored their survival. Offspring from hermaphrodite mothers exposed to *E. coli* scent served as the control group. As shown in **Supplementary Fig. 2**, the survival of F1 animals does not significantly differ from the control group; however, a slight upward trend is observed. To investigate this further, we conducted a more detailed analysis by examining the data for each biological replicate individually. We observed that F1 animals exhibited increased survival when their mothers originated from populations (biological replicates) with a higher average number of exophers and stronger responses to PA14 scent. Consequently, we categorized our data into two groups based on two criteria: (i) populations with more or fewer than 7 exophers on average in the P0 generation, and (ii) populations where P0 worms exposed to PA14 produced more or fewer than 10 exophers. As illustrated in **Fig. 8e**, F1 animals from the high exopher-producing group exhibited significantly longer survival following infection (while P0 animals lived significantly shorter lives) compared to control F1 animals. In contrast, there was no statistically significant difference in survival between the low exopher-producing group and the control group for either the P0 or F1 generations (**Fig. 8f**). These findings suggest that when hermaphrodite mothers produce a large number of exophers in response to pathogen-derived volatile metabolites, their offspring exhibit enhanced survival, albeit at the cost of maternal survival.

Model of exopher regulation mechanism in *C. elegans*

Based on our investigations, we propose the following model outlining the complex mechanism of exopher regulation by pathogen-derived metabolites (**Fig. 9**):

1. Pathogen-induced exopher production: Exposure to live *Pseudomonas aeruginosa* PA14 or *Serratia marcescens* Db10 induces exopher production in *C. elegans* body wall muscles.
2. Immune pathway involvement: The production of exophers is influenced by key immune pathways (insulin, TGFβ, p38 MAPK, and IPR), although pathogen-induced exophergenesis occurs in most immune mutants.
3. Non-volatile and volatile pathogen metabolites: Both non-volatile (supernatant) and volatile pathogen metabolites trigger exopher production, with distinct sensory neurons (ADL, ASK, AWC) involved in regulation. Neurons such as ASI, ASH, and AWB regulate non-volatile metabolite-induced exopher production but not volatile metabolite-induced production.
4. Involvement of GPCRs: Neuronally-expresssed and non neuronally-expressed GPCRs *sri-36*, *sri-39*, *sri-19*, and *srr-6* play key roles in inducing exophergenesis upon exposure to pathogen non-volatile metabolites.
5. Offspring survival and maternal cost: Offspring of mothers producing many exophers in response to pathogen metabolites exhibit increased survival during infection, while the mothers themselves experience reduced survival, indicating a trade-off between maternal survival and offspring fitness.

Discussion

Our findings suggest that, although exophers produced in response to different stimuli may appear similar in number, the distinct signalling pathways involved indicate potential differences in their roles or contents. Specifically, supernatant-induced exopher production, which depends on immune pathways such as p38 MAPK and TGF-β, differs from volatile-

induced exopher production, which appears to operate independently of these pathways. This distinction implies that exophers may constitute distinct subtypes of EVs with unique molecular compositions and functions. The possibility that quantitatively similar exophers could be functionally distinct opens new research avenues to isolate and characterize these vesicles in detail. By analysing their content in response to both volatile and non-volatile metabolites, we could uncover their specific roles in organismal health and pathogen defence. Our results further reveal that the mechanisms triggering exopher production are influenced by the type of metabolite detected: non-volatile pathogen metabolites, signalling a more immediate threat, activate immune pathways to induce exopher production, while volatile metabolites, which suggest the pathogen is nearby but not directly infecting, bypass these immune pathways. This discrepancy underscores the complexity of the worm's physiological responses to environmental cues, suggesting that exopher production is finely regulated based on the nature of the perceived threat. Consequently, non-volatile metabolite-induced exophers may play a more immediate role in worms physiology, while volatile-induced exophers could serve to prepare the organism for future stressors.

Previous studies have shown that increased exopher release can benefit the organism by removing protein aggregates[13], extending lifespan[16], or promoting faster offspring development[14]. However, when exopher release is elevated in response to pathogen exposure, we observe an opposite effect, leading to decreased survival upon infection. This suggests that exophers, or possibly EV in general, may function under a hormetic response: while a moderate increase in EV production appears beneficial, an excessive increase may overwhelm the organism, negating any positive effects. Thus, while moderate exopher production may be beneficial, too much exopher release might impose a burden on the organism, potentially due to changes in the content of these vesicles under different environmental conditions.

Interestingly, while volatile metabolites like 1-undecene have been shown to increase lifespan in *C. elegans* under non-pathogenic conditions[46] or to protects worms against a subsequent infection with *P. aeruginosa*[31], our results demonstrate that volatile-induced exopher production can lead to decreased survival during infection. The differences in the type, timing, and context of exposure likely contribute to this contradiction. In previous studies, a specific compound and shorter exposure periods were used. In contrast, our study involved prolonged exposure to a mixture of volatile metabolites from pathogens, which may trigger different physiological responses. The involvement of multiple G protein-coupled receptors (GPCRs) in regulating exopher production suggests that exophergenesis is not triggered by a single metabolite but by a complex cocktail of pathogen-derived signals. This complexity may allow the organism to fine-tune its response depending on the nature of the threat it perceives, enabling a more nuanced and context-dependent reaction to environmental challenges.

In conclusion, our study highlights the complexity of exopher production in response to pathogen-derived signals. The ability of *C. elegans* to detect and respond to volatile and non-volatile metabolites in a context-dependent manner suggests that exophers and other EVs play a crucial role in mediating the organism's physiological response to environmental stressors. Future research should focus on isolating and characterizing exophers produced under different conditions to determine their specific molecular contents and functions. Understanding how these vesicles contribute to both the short-term survival of the organism and the long-term fitness of its offspring will provide deeper insights into the adaptive roles of EVs in host-pathogen interactions as well as in animals healthspan and lifespan.

Methods

Worm Maintenance and Strains

C. elegans strains were maintained at 20°C on nematode growth medium (NGM) plates seeded with *Escherichia coli* OP50 as a food source[47]. Only hermaphrodites were used in the experiments. A comprehensive list of all chemicals and strains used in the study are provided in Supplementary Table 1 and 2, respectively.

Pathogen procedures

Pathogen bacteria media plates preparation

Worms were exposed to either *Pseudomonas aeruginosa* PA14 or *Serratia marcescens* Db10 strains. Pathogen-seeded plates were prepared following standard protocols[48,49].

The PA14 strain was revived from frozen stock by streaking onto a 10-cm LB agar plate and incubating at 37°C for 12–18 hours. Plates were stored at 4°C and used within one week. A single PA14 colony was inoculated into 5 mL of LB broth and incubated overnight (maximum 16 hours) at 37°C with shaking at 250 rpm. Following incubation, 10 µL of the overnight PA14 culture was spotted onto the center of 35 mm "slow killing" plates (SK plates), which were incubated at 37°C for 24 hours, followed by 25°C for another 24 hours to maximize virulence.

For *S. marcescens* Db10, the strain was similarly streaked from frozen stock onto a 10-cm LB agar plate, incubated at 37°C for 12–18 hours, and stored at 4°C for up to one week. A single Db10 colony was inoculated into 5 mL of LB broth and cultured at 37°C with shaking for 8–10 hours. To prepare NGM infection plates, 25 µL of the *S. marcescens* culture was seeded onto 35 mm NGM plates, which were incubated at 37°C overnight.

All the experiments with the pathogenic bacteria were conducted in Biosafety level 2 laboratory.

Short time infection assay

Worms were age-synchronized by isolating pretzel-stage embryos. Upon reaching the first day of adulthood (AD1), they were transferred either to control plates seeded with *E. coli* OP50 or to plates seeded with the pathogens PA14 or Db10. Worms were exposed directly to the pathogens for 3 hours at 20°C, after which they were transferred back to OP50 seeded plates. Exopher levels were assessed the following day, on the second day of adulthood (AD2).

Pathogen supernatant assay

To collect non-volatile metabolites, a single colony of PA14 was inoculated into 5 mL of LB media and cultured overnight for a maximum of 16 hours at 37°C. After incubation, bacterial cells were removed by passing the culture through a 0.22 μm filter, and the bacterial supernatant was collected. Age-synchronized L4 stage worms (n = 30), grown on 60 mm NGM plates seeded with OP50, were treated with 50 μL of the filtered bacterial supernatant, while control worms received 50 μL of LB broth. Plates were sealed with parafilm, and exophers were scored 48 hours later, when the worms reached AD2.

Volatile metabolites chamber assay

Pretzel-stage embryos were placed on 35-mm NGM plates seeded with *E. coli* OP50, with 10 embryos per plate. Once the embryos developed into L4 stage worms, a chamber with volatile metabolites was assembled by placing a 35 mm SK plate containing PA14 or a control 35 mm NGM plate with OP50 on the bottom. The plate with synchronized worms was positioned on top, and the two plates were sealed together with parafilm. Worms were incubated with volatile metabolites of the bacteria for 48h hours. Exophers were evaluated at the second day of adulthood.

Offspring survival assay

The parental generation (P0 generation) of *C. elegans* was synchronized by placing 10 pretzel-stage embryos on 35 mm NGM plates seeded with OP50. As described in the "Volatile Metabolites Chamber Assay," chambers were assembled using either OP50 or PA14 when the worms reached the L4 stage. After 48 hours of exposure to volatile metabolites, exophers were scored in the parental generation on the AD2.

Next, pretzel-stage embryos (F1 generation) of the P0 exposed to OP50 or PA14 volatiles were collected and placed on 35 mm NGM plates seeded with OP50 (15 embryos per plate). When the F1 worms reached the L4 stage, they were infected according to the standard infection assay (references). L4 larvae were transferred to SK plates and incubated at 25°C. FUdR was not included in the plates.

The survival of the F1 population was monitored at multiple time points using a touch movement assay. Worms that failed to respond to touch were scored as dead, removed from the killing plates, and recorded. Worms that responded to touch were scored as alive and also counted. Survival was recorded at least twice daily until the entire population had died.

Egg retention assay

First, AD1 age-synchronized worms were placed on either a lawn of pathogenic bacteria (PA14 and Db10) or a control lawn of OP50 for 3 hours. After exposure, worms were transferred to OP50 plates and cultured until they reached the AD2 stage. In the next step, hermaphrodites were treated with 1.8% hypochlorite solution. Once the worms dissolved, the embryos retained in the uterus were counted.

RNA Interference Assay

RNA interference (RNAi) in *C. elegans* was performed using the standard RNAi feeding method[50]. Briefly, RNAi plates were prepared by supplementing NGM with 12.5 μg/mL

tetracycline, 100 µg/mL ampicillin, and 1 mM IPTG. These plates were seeded with *E. coli* HT115 bacteria expressing double-stranded RNA (dsRNA) targeting the gene of interest. Control worms were fed *E. coli* HT115 containing the empty vector L4440.

Age-synchronized pretzel-stage embryos were transferred onto the freshly prepared RNAi plates and cultured until day 2 of adulthood, at which point exophers were quantified. The developmental stage of the worms was confirmed at the L4 stage, and any individuals that were developmentally advanced or delayed were excluded from the experiment.

Transcriptome analysis

C. elegans RNA extractions, library preparations, and sequencing were performed by Azenta US, Inc (South Plainfield, NJ, USA) as follows:

RNA extraction

Total RNA was extracted using Qiagen RNeasy Plus mini kit (Qiagen, Hilden, Germany) following the manufacturer's instructions.

Library preparation with polyA selection and Illumina sequencing

RNA samples were quantified using the Qubit 2.0 Fluorometer (Life Technologies, Carlsbad, CA, USA), and their integrity was assessed with the Agilent TapeStation 4200 (Agilent Technologies, Palo Alto, CA, USA). RNA sequencing libraries were constructed using the NEBNext Ultra II RNA Library Prep Kit for Illumina, following the manufacturer's protocol (NEB, Ipswich, MA, USA). In brief, mRNA was enriched using Oligo(dT) beads and subsequently fragmented at 94°C for 15 minutes. First and second-strand cDNA synthesis was performed, followed by end repair and adenylation of the cDNA fragments at their 3' ends. Universal adapters were then ligated to the cDNA fragments, and libraries were enriched through a limited-cycle PCR with the addition of indexing sequences. The resulting sequencing

libraries were validated using the Agilent TapeStation and quantified with both the Qubit 2.0 Fluorometer (Invitrogen, Carlsbad, CA, USA) and quantitative PCR (KAPA Biosystems, Wilmington, MA, USA). The libraries were multiplexed and loaded onto the Illumina NovaSeq 6000 platform according to the manufacturer's instructions. Sequencing was performed with a 2×150 paired-end (PE) configuration using v1.5 reagents. Image analysis and base calling were carried out using the NovaSeq Control Software v1.7. The raw sequence data (.bcl files) generated were converted into fastq files and de-multiplexed using the Illumina bcl2fastq software (version 2.20), allowing for one mismatch in index sequence identification.

Sequencing data analysis

Following quality assessment of the raw sequencing data, reads were trimmed to remove potential adapter sequences and low-quality nucleotides using Trimmomatic v0.36. The cleaned reads were then aligned to the Caenorhabditis elegans reference genome from ENSEMBL using the STAR aligner v2.5.2b. STAR is a splice-aware aligner that identifies splice junctions and integrates them into the alignment process to enhance the accuracy of read mapping. This step resulted in the generation of BAM files. Unique gene hit counts were calculated using the featureCounts function from the Subread package v1.5.2, considering only reads uniquely aligned to exon regions.

The gene hit counts were subsequently used for downstream differential expression analysis. DESeq2 was employed to compare gene expression levels between different sample groups. The Wald test was used to calculate p-values and log2 fold changes. Genes with an adjusted p-value < 0.05 and an absolute log2 fold change > 1 were considered differentially expressed in each comparison.

Scoring of Exophers and Fluorescence Microscopy

Exopher quantification was performed as described in Turek et al.[14] and Banasiak et al.[20] (Bio-Protocol, detailed, step-by-step guide). In brief, exophers were scored using a Zeiss Axio Zoom.V16 stereomicroscope equipped with filter sets 63 HE and 38 HE. Worms were age-synchronized by isolating pretzel-stage embryos and maintained until day 2 of adulthood. On the second day of adulthood, worms were observed on NGM plates, and the number of exophers per freely moving worm was recorded.

Representative fluorescence images were captured using a Zeiss LSM800 laser-scanning confocal microscope equipped with a 40× oil immersion objective. GFP and RFP fluorescence were excited using 488 nm and 561 nm lasers, respectively. For imaging, worms were immobilized on 5% agarose pads, using either 10 µl of PolySciences 0.05 µm polystyrene microspheres or 25 µM tetramisole as an anesthetic.

Generation of *sri-19, sri-36/39,* and *srr-6* mutant strains

CRISPR/Cas9 genome editing was employed to generate the *sri-19* mutants (*sri-19(wwa15)* and *sri-19(wwa16)*) following previously established protocols[51]. The crRNA sequence used to target the *sri-19* locus was ATAATTGGTGGATATACAAATGG. Mutations were mapped to the first exon, resulting in frame shifts that likely produce molecular null alleles.

To create *srr-6* mutants, a previously described STOP-IN strategy[52] was used, which introduces an early stop codon within the first exon. The crRNA sequence used to target the *srr-6* locus was ACTCCAAGTCCTGAAGTCGT, and the STOP-IN cassette sequence was GGGAAGTTTGTCCAGAGCAGAGGTGACTAAGTGATAA, flanked by AATCTTTTTCAACAATGATTACTCCAAGTCCTGAAGTCGT (left) and GGGTGACGAGGTTTCGTGTCCATCTATTATTGAAATACCT (right).

For the deletion of both the *sri-36* and *sri-39* genes, the entire 5968 bp region encompassing both genes (including the intercalated gene F33H12.7) was removed and replaced with a STOP-IN cassette (GGGAAGTTTGTCCAGAGCAGAGGTGACTAAGTGATAA). The flanking sequences were TGGTTACTTTTTATTTTTATTTTTC (left) and AATCCTAATCTAATATGAATCAATT (right). The crRNA sequences used for this deletion were ACAATGCTAGTTGTAGGTAC and ATTCATATTAGATTAGGATT.

All mutant strains were backcrossed twice with N2 wild-type worms to remove background mutations and verified using Sanger sequencing.

Data Analysis and Visualization

Data analysis was performed using Microsoft Excel and GraphPad Prism 9. Graphical representations of the results were generated in GraphPad Prism 9.

Statistical Analysis

No prior statistical methods were applied to determine sample sizes. Worms were randomly allocated to experimental groups, and all experiments were conducted in a blinded fashion for the datasets presented in Figures 2, 3, 4, 5, 7, and 8. Given the assumption of non-Gaussian distribution of residuals, nonparametric statistical tests were employed. For pairwise comparisons, two-tailed Mann–Whitney tests were used, while Kruskal-Wallis tests followed by Dunn's multiple comparisons test were applied for multi-group comparisons. A p-value of < 0.05 was considered statistically significant.

References

1. Buzas, E. I. The roles of extracellular vesicles in the immune system. *Nat. Rev. Immunol.* **23**, 236–250 (2023).

2. Robbins, P. D. & Morelli, A. E. Regulation of immune responses by extracellular vesicles. *Nat. Rev. Immunol.* **14**, 195–208 (2014).

3. Peregrino, E. S. *et al.* The Role of Bacterial Extracellular Vesicles in the Immune Response to Pathogens, and Therapeutic Opportunities. *International Journal of Molecular Sciences* vol. 25 (2024).

4. Berumen Sánchez, G., Bunn, K. E., Pua, H. H. & Rafat, M. Extracellular vesicles: mediators of intercellular communication in tissue injury and disease. *Cell Commun. Signal.* **19**, 104 (2021).

5. Naznin, H. A. *et al.* Systemic Resistance Induced by Volatile Organic Compounds Emitted by Plant Growth-Promoting Fungi in Arabidopsis Thaliana. *PLoS One* **9**, e86882 (2014).

6. McEwan, D. L., Kirienko, N. V & Ausubel, F. M. Host Translational Inhibition by Pseudomonas Aeruginosa Exotoxin a Triggers an Immune Response in Caenorhabditis Elegans. *Cell Host Microbe* **11**, 364–374 (2012).

7. Marsh, E. K. & May, R. C. *Caenorhabditis elegans*, a Model Organism for Investigating Immunity. *Appl. Environ. Microbiol.* **78**, 2075–2081 (2012).

8. Irazoqui, J. E., Urbach, J. M. & Ausubel, F. M. Evolution of host innate defence: insights from Caenorhabditis elegans and primitive invertebrates. *Nat. Rev. Immunol.* **10**, 47–58 (2010).

9. Peterson, N. D. & Pukkila-Worley, R. Caenorhabditis elegans in high-throughput screens for anti-infective compounds. *Curr. Opin. Immunol.* **54**, 59–65 (2018).

10. Iwama, R. E. & Moran, Y. Origins and diversification of animal innate immune responses against viral infections. *Nat. Ecol. Evol.* **7**, 182–193 (2023).

11. Harding, B. W. & Ewbank, J. J. An integrated view of innate immune mechanisms in C. elegans. *Biochem. Soc. Trans.* **49**, 2307–2317 (2021).

12. Wang, J., Barr, M. M. & Wehman, A. M. Extracellular vesicles. *Genetics* **227**, (2024).

13. Melentijevic, I. *et al.* C. elegans neurons jettison protein aggregates and mitochondria under neurotoxic stress. *Nature* **542**, 367–371 (2017).

14. Turek, M. *et al.* Muscle-derived exophers promote reproductive fitness. *EMBO Rep.* e52071 (2021) doi:10.15252/embr.202052071.

15. Arnold, M. L. *et al.* Intermediate filaments associate with aggresome-like structures in proteostressed C. elegans neurons and influence large vesicle extrusions as exophers. *Nat. Commun.* **14**, 4450 (2023).

16. Yang, Y. *et al.* Autophagy protein ATG-16.2 and its WD40 domain mediate the beneficial effects of inhibiting early-acting autophagy genes in C. elegans neurons. *Nat. aging* (2024) doi:10.1038/s43587-023-00548-1.

17. Cooper, J. F., Guasp, R. J., Arnold, M. L., Grant, B. D. & Driscoll, M. Stress increases in exopher-mediated neuronal extrusion require lipid biosynthesis, FGF, and EGF RAS/MAPK signaling. *Proc. Natl. Acad. Sci.* **118**, e2101410118 (2021).

18. Szczepańska, A. *et al.* Pheromone-based communication influences the production of somatic extracellular vesicles in C. elegans. *Nat. Commun.* **15**, 2715 (2024).

19. Nicolás-Ávila, J. A. *et al.* A Network of Macrophages Supports Mitochondrial Homeostasis in the Heart. *Cell* **183**, 94-109.e23 (2020).

20. Banasiak, K., Turek, M. & Pokrzywa, W. Preparation of Caenorhabditis elegans for Scoring of Muscle-derived Exophers. *Bio-protocol* **13**, (2023).

21. Schorey, J. S., Cheng, Y., Singh, P. P. & Smith, V. L. Exosomes and other extracellular vesicles in host–pathogen interactions. *EMBO Rep.* **16**, 24–43 (2015).

22. Kim, D. H. Signaling in the innate immune response. *WormBook* **2018**, 1–35 (2018).

23. Martineau, C. N., Kirienko, N. V & Pujol, N. Innate immunity in C. elegans. *Curr. Top. Dev. Biol.* **144**, 309–351 (2021).

24. Murphy, C. T. & Hu, P. J. Insulin/insulin-like growth factor signaling in C. elegans. *WormBook* 1–43 (2013) doi:10.1895/wormbook.1.164.1.

25. Gumienny, T. L. & Savage-Dunn, C. TGF-β signaling in C. elegans. *WormBook* 1–34 (2013) doi:10.1895/wormbook.1.22.2.

26. Kim, D. H. *et al.* A conserved p38 MAP kinase pathway in Caenorhabditis elegans innate immunity. *Science* **297**, 623–626 (2002).

27. Liberati, N. T. *et al.* Requirement for a conserved Toll/interleukin-1 resistance domain protein in the Caenorhabditis elegans immune response. *Proc. Natl. Acad. Sci. U. S. A.* **101**, 6593–6598 (2004).

28. Lažetić, V., Batachari, L. E., Russell, A. B. & Troemel, E. R. Similarities in the induction of the intracellular pathogen response in Caenorhabditis elegans and the type I interferon response in mammals. *BioEssays* **45**, 2300097 (2023).

29. Balla, K. M. & Troemel, E. R. aenorhabditis elegans as a model for intracellular pathogen infection. *Cell. Microbiol.* **15**, 1313–1322 (2013).

30. Wang, G. *et al.* Mechanical force of uterine occupation enables large vesicle extrusion from proteostressed maternal neurons. *Elife* **13**, RP95443 (2024).

31. Prakash, D. *et al.* 1-Undecene from Pseudomonas aeruginosa is an olfactory signal for flight-or-fight response in Caenorhabditis elegans. *EMBO J.* **40**, e106938 (2021).

32. Dishart, J. G. *et al.* Olfaction regulates peripheral mitophagy and mitochondrial function. *Sci. Adv.* **10**, eadn0014 (2024).

33. Peterson, N. D. *et al.* Non-canonical pattern recognition of a pathogen-derived metabolite by a nuclear hormone receptor identifies virulent bacteria in C. elegans. *Immunity* **56**, 768-782.e9 (2023).

34. Ferkey, D. M., Sengupta, P. & L'Etoile, N. D. Chemosensory signal transduction in Caenorhabditis elegans. *Genetics* **217**, iyab004 (2021).

35. Filipowicz, A., Lalsiamthara, J. & Aballay, A. Dissection of a sensorimotor circuit underlying pathogen aversion in C. elegans. *BMC Biol.* **20**, 229 (2022).

36. Styer, K. L. *et al.* Innate Immunity in Caenorhabditis elegans Is Regulated by Neurons Expressing NPR-1/GPCR. *Science (80-.).* **322**, 460–464 (2008).

37. Foster, K. J. *et al.* Innate Immunity in the C. elegans Intestine Is Programmed by a Neuronal Regulator of AWC Olfactory Neuron Development. *Cell Rep.* **31**, 107478 (2020).

38. White, J. G., Southgate, E., Thomson, J. N. & Brenner, S. The structure of the nervous system of the nematode Caenorhabditis elegans. *Philos. Trans. R. Soc. London. Ser. B, Biol. Sci.* **314**, 1–340 (1986).

39. Yu, Y., Zhi, L., Wu, Q., Jing, L. & Wang, D. NPR-9 regulates the innate immune response in Caenorhabditis elegans by antagonizing the activity of AIB interneurons. *Cell. Mol. Immunol.* **15**, 27–37 (2018).

40. Reboul, J. & Ewbank, J. J. GPCRs in invertebrate innate immunity. *Biochem. Pharmacol.* **114**, 82–87 (2016).

41. Dubyak, G. R. Chapter 21 - GPCRs in innate and adaptive immune responses. in (eds. Jastrzebska, B. & Park, P. S.-H. B. T.-Gpcr.) 429–461 (Academic Press, 2020). doi:https://doi.org/10.1016/B978-0-12-816228-6.00021-0.

42. Sellegounder, D. *et al.* Neuronal GPCR NPR-8 regulates C. elegans defense against pathogen infection. *Sci. Adv.* **5**, eaaw4717 (2024).

43. Vidal, B. *et al.* An atlas of Caenorhabditis elegans chemoreceptor expression. *PLOS Biol.* **16**, e2004218 (2018).

44. Szczepanska, A. *et al.* Data accompanying the manuscript Pheromone-based communication influences the production of somatic extracellular vesicles in C. elegans. (2024) doi:10.5281/zenodo.10718535.

45. Eder, M. *et al.* Systematic mapping of organism-scale gene-regulatory networks in aging using population asynchrony. *Cell* (2024) doi:10.1016/j.cell.2024.05.050.

46. De-Souza, E. A., Thompson, M. A. & Taylor, R. C. Olfactory chemosensation extends lifespan through TGF-β signaling and UPR activation. *Nat. Aging* (2023) doi:10.1038/s43587-023-00467-1.

47. Brenner, S. The genetics of Caenorhabditis elegans. *Genetics* **77**, 71–94 (1974).

48. Foster, K. J., McEwan, D. L. & Pukkila-Worley, R. Measurements of Innate Immune Function in C. elegans. *Methods Mol. Biol.* **2144**, 145–160 (2020).

49. Powell, J. R. & Ausubel, F. M. Models of Caenorhabditis elegans Infection by Bacterial and Fungal Pathogens BT - Innate Immunity. in (eds. Ewbank, J. & Vivier, E.) 403–427 (Humana Press, 2008). doi:10.1007/978-1-59745-570-1_24.

50. Kamath, R. S. & Ahringer, J. Genome-wide RNAi screening in Caenorhabditis elegans. *Methods* **30**, 313–321 (2003).

51. Dokshin, G. A., Ghanta, K. S., Piscopo, K. M. & Mello, C. C. Robust Genome Editing with Short Single-Stranded and Long, Partially Single-Stranded DNA Donors in Caenorhabditis elegans. *Genetics* **210**, 781–787 (2018).

52. Wang, H., Park, H., Liu, J. & Sternberg, P. W. An Efficient Genome Editing Strategy To Generate Putative Null Mutants in Caenorhabditis elegans Using CRISPR/Cas9. *G3 (Bethesda).* **8**, 3607–3616 (2018).

53. Taylor, S. R. *et al.* Molecular topography of an entire nervous system. *Cell* **184**, 4329-4347.e23 (2021).

Acknowledgements

Some strains were provided by the CGC, which is funded by NIH Office of Research Infrastructure Programs (P40 OD010440). We thank Monika Woźniak, Natalia Wasiak,

Małgorzata Śledź, Tomasz Strumiński for assistance with worms maintenance; Adam Kłosin for discussions and comments on the manuscript. Work in the MT Laboratory was mainly funded by a National Science Centre SONATA grant (2019/35/D/NZ3/04091 to MT) and additionally supported by a National Science Centre SONATA BIS grant (2021/42/E/NZ3/00358 to MT). Work in the WP Laboratory was funded by the Norwegian Financial Mechanism 2014-2021 operated by the Polish National Science Centre, Poland (project contract number 2019/34/H/NZ3/00691 to WP).

Author Contributions

Conceptualization: MT; Data curation: MT; Formal analysis: KK, AS, MT, WP, NP; Funding acquisition: MT, WP, NP; Investigation: KK, AS, MT; Methodology: MT, NP, WP, KK, AS; Project administration: MT; Resources: MT, NP, WP; Supervision: MT, NP; Validation: MT, WP, KK, AS, NP; Visualization: KK, AS, MT; Writing – original draft: MT; Writing – review & editing: MT, WP, KK, AS, NP.

Competing Interests

The authors declare no competing interests.

Figures and Figure Legends

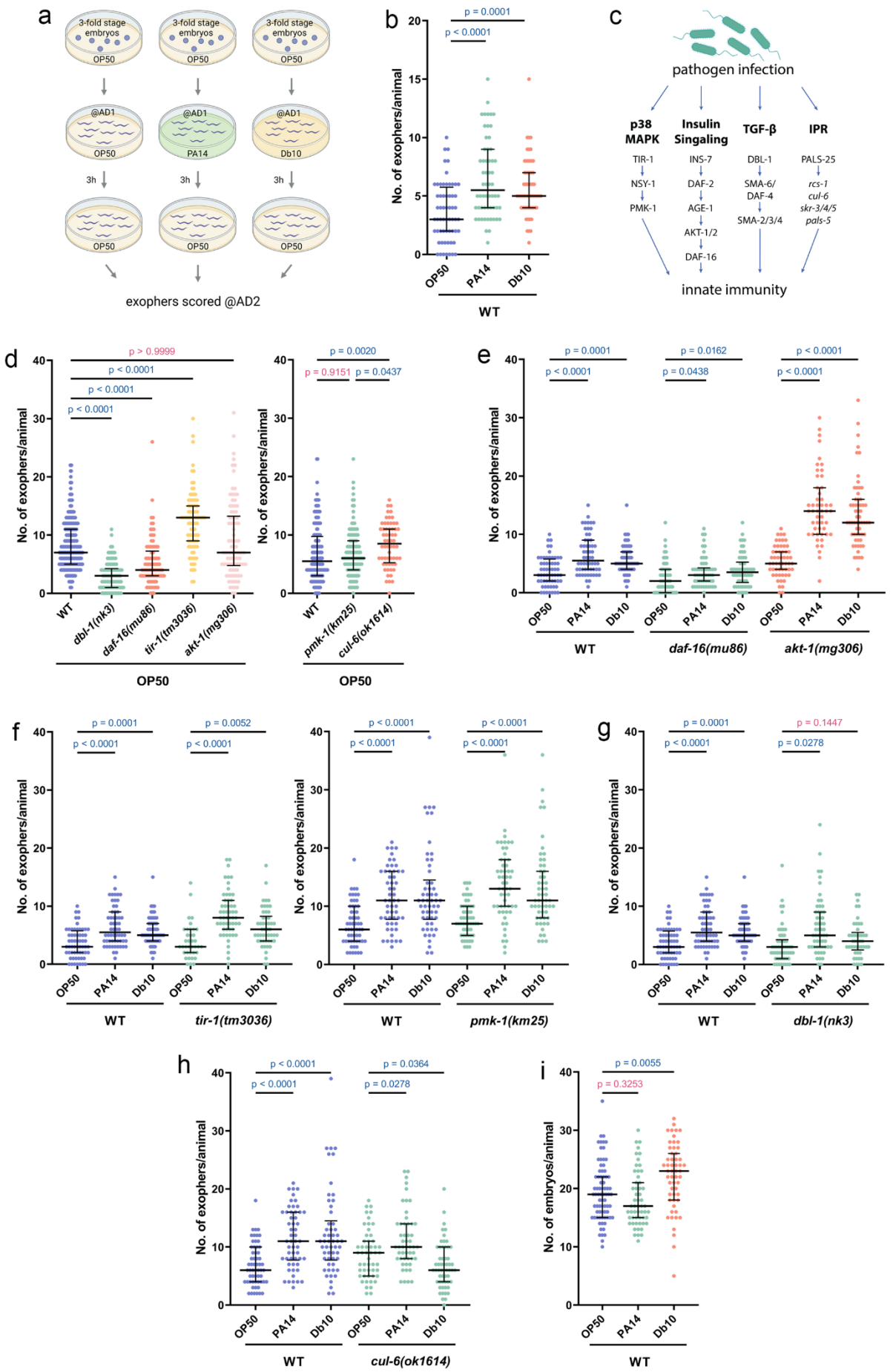
a
3-fold stage embryos
OP50
@AD1
PA14
Db10
3h
exophers scored @AD2
b
No. of exophers/animal
p = 0.0001
p < 0.0001
OP50
PA14
Db10
WT
c
pathogen infection
p38 MAPK
Insulin Singaling
TGF-β
IPR
TIR-1
NSY-1
PMK-1
INS-7
DAF-2
AGE-1
AKT-1/2
DAF-16
DBL-1
SMA-6/ DAF-4
SMA-2/3/4
PALS-25
rcs-1
cul-6
skr-3/4/5
pals-5
innate immunity
d
p > 0.9999
p < 0.0001
p = 0.0020
p = 0.9151
p = 0.0437
WT
dbl-1(nk3)
daf-16(mu86)
tir-1(tm3036)
akt-1(mg306)
pmk-1(km25)
cul-6(ok1614)
e
p = 0.0162
p = 0.0438
f
p = 0.0052
g
p = 0.1447
p = 0.0278
h
p = 0.0364
i
No. of embryos/animal
p = 0.3253

Figure 1. Production of *C. elegans* muscle exophers is upregulated during pathogen infection.

a Experimental Setup: Synchronized AD1 worms were exposed to *Pseudomonas aeruginosa* (PA14) and *Serratia marcescens* (Db10), or to *Escherichia coli* (OP50) for 3 hours at 20°C, followed by transfer to OP50-seeded plates. Exopher production was assessed on the second day of adulthood (AD2). Created with BioRender.com.

b Short time infection with *P. aeruginosa* PA14 or *S. marcescens* Db10 leads to increased exopher production (n = 60 worms, N = 2 independent experiments).

c Investigated innate immunity pathways: Various innate immunity pathways were assessed for their roles in regulating exopher production.

d Worms deficient in key immune response pathways exhibited changes in exopher levels (n = 90 worms, N = 3 independent experiments; n = 90-180 worms, N = 3-6 independent experiments).

e - g Infection-induced exopher production is not dependent on the (e) insulin signalling, (f) p38 MAPK, or (g) TGF-β pathways pathway (n = 37-60 worms, N = 2 independent experiments). The data shown in graphs e–h were collected together and share the same controls but are presented in separate panels to improve visualization and enhance clarity.

h Exopher production in response to *S. marcescens* Db10 infection is fully dependent on the IPR pathway, while production in response to *P. aeruginosa* PA14 infection is partially dependent on this pathway (n = 51-58 worms, N = 2 independent experiments). The data shown in graphs e–h were collected together and share the same controls but are presented in separate panels to improve visualization and enhance clarity.

i Exposure to *S. marcescens* Db10, but not *P. aeruginosa* PA14, results in embryo retention in the uterus (n = 54-75 worms, N = 3-4 independent experiments).

Data are presented as medians with interquartile ranges. Non-significant p-values ($p > 0.05$) are highlighted in pink, while significant p-values ($p < 0.05$) are shown in blue. Statistical significance was assessed using the Kruskal-Wallis test with Dunn's multiple comparisons test.

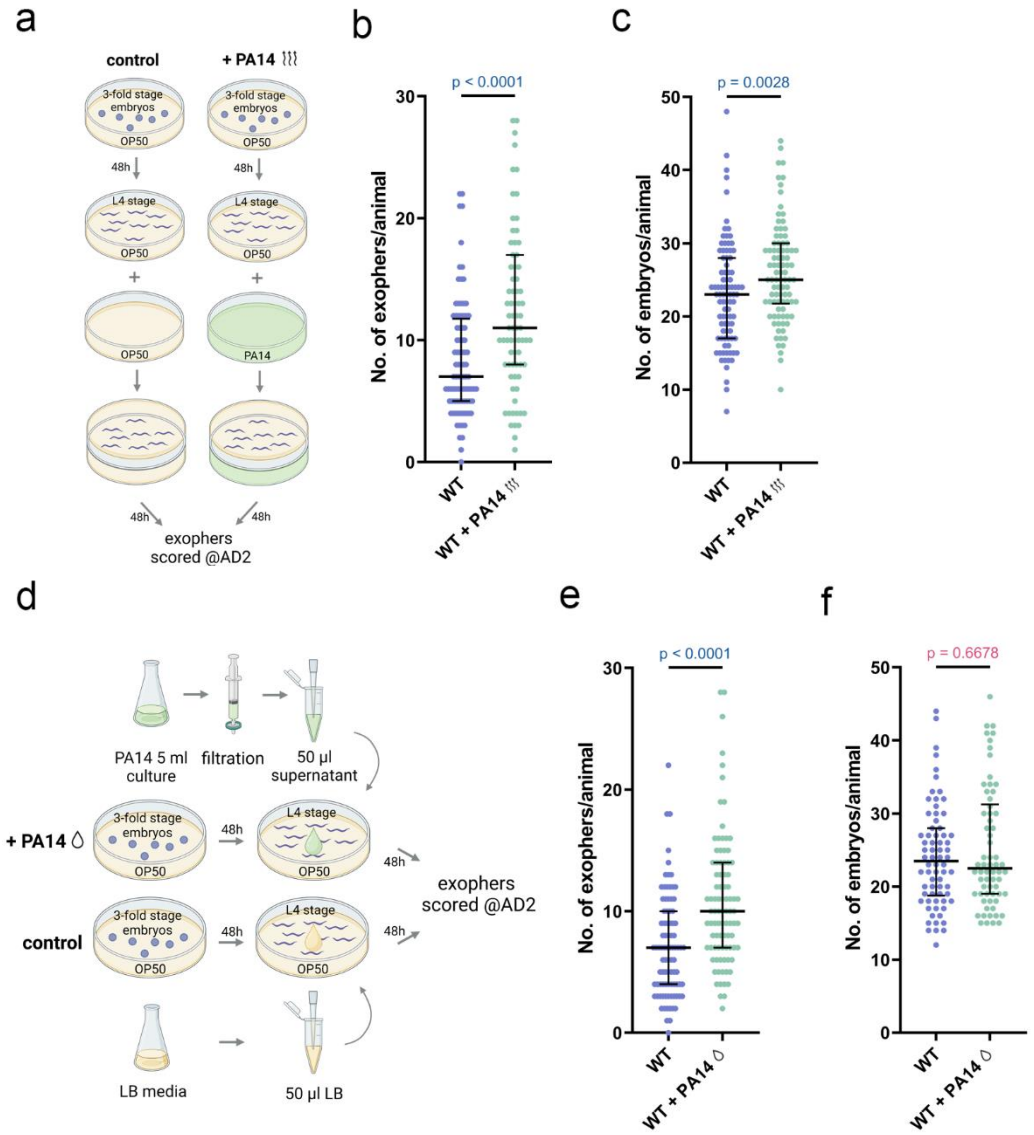

Figure 2. The production of muscle exophers in *C. elegans* is regulated by both volatile and non-volatile metabolites from pathogens.

a Experimental setup schematic: Synchronized L4-stage worms were exposed to PA14 volatile metabolites or OP50 for 48 hours, and exopher production was evaluated on the second day of adulthood (AD2). Created with BioRender.com.

b Exposure to PA14 volatile metabolites significantly increases exopher levels in worms (n = 77-90 worms, N = 3 independent experiments).

c Volatile metabolites exposure causes embryo retention in the uterus (n = 90 worms, N = 3 independent experiments).

d Experimental setup schematic: L4-stage worms were exposed to 50 μL of filtered pathogen supernatant, while controls received 50 μL of LB broth. Exophers were scored after 48 hours, at AD2.

e Exposure to PA14 supernatant results in increased exopher production (n = 90 worms, N = 3 independent experiments).

f PA14 supernatant exposure does not induce embryo retention (n = 67-70 worms, N = 3 independent experiments).

Data are presented as medians with interquartile ranges. Statistical analyses were performed using the two-tailed Mann-Whitney test, with non-significant p-values ($p > 0.05$) in pink and significant p-values ($p < 0.05$) in blue.

a

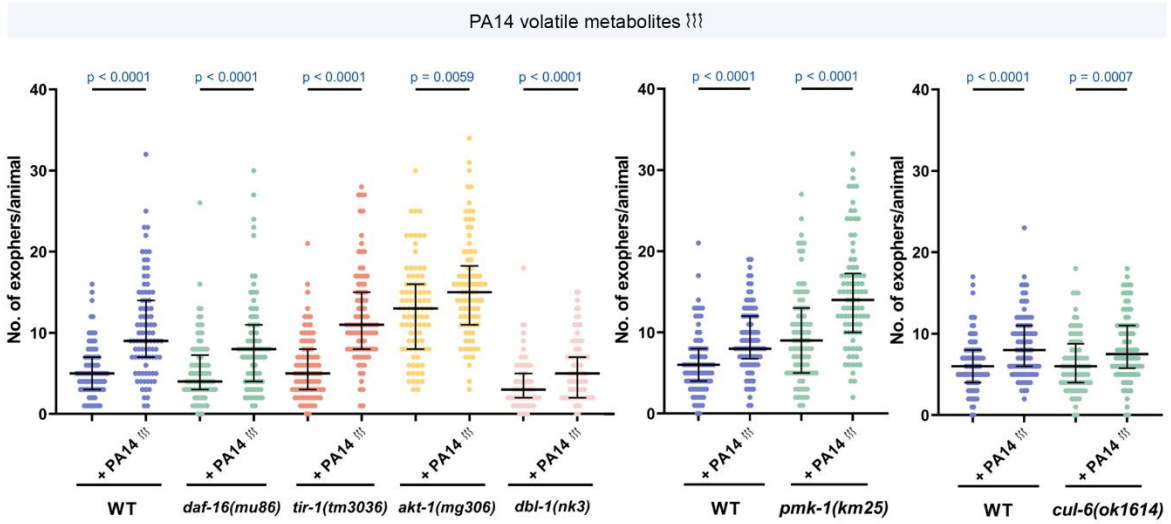

b

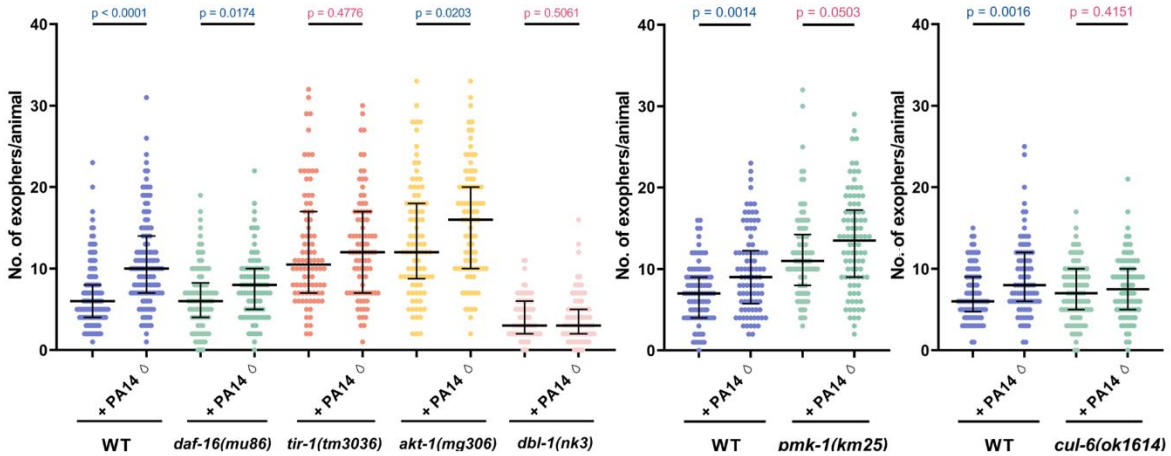

c

	genes of the pathway	PA14 volatile metabolites	PA14 supernatant
p38 MAPK	*tir-1*	p < 0.0001	p = 0.4776
	pmk-1	p < 0.0001	p = 0.0503
Insulin Signaling	*akt-1*	p = 0.0059	p = 0.0203
	daf-16	p < 0.0001	p = 0.0174
TGF-β	*dbl-1*	p < 0.0001	p = 0.5061
IPR	*cul-6*	p = 0.0007	p = 0.4151

Figure 3. Exopher production in response to pathogen volatile metabolites and supernatant is governed by distinct regulatory mechanisms.

a Increased exopher production after exposure to PA14 volatile metabolites does not depend on innate immunity pathways (n = 80-90 worms, N = 3 independent experiments).

b Increased exopher production after exposure to PA14 non-volatile metabolites depends on p38, TGF-β, and IPR pathways (n = 85-120 worms, N = 3-4 independent experiments).

c Summary of experimental results: A table summarizing the experimental findings, including p-values. Created with BioRender.com.

Data are presented as medians with interquartile ranges. Statistical analyses were performed using the two-tailed Mann-Whitney test, with non-significant p-values ($p > 0.05$) in pink and significant p-values ($p < 0.05$) in blue.

a

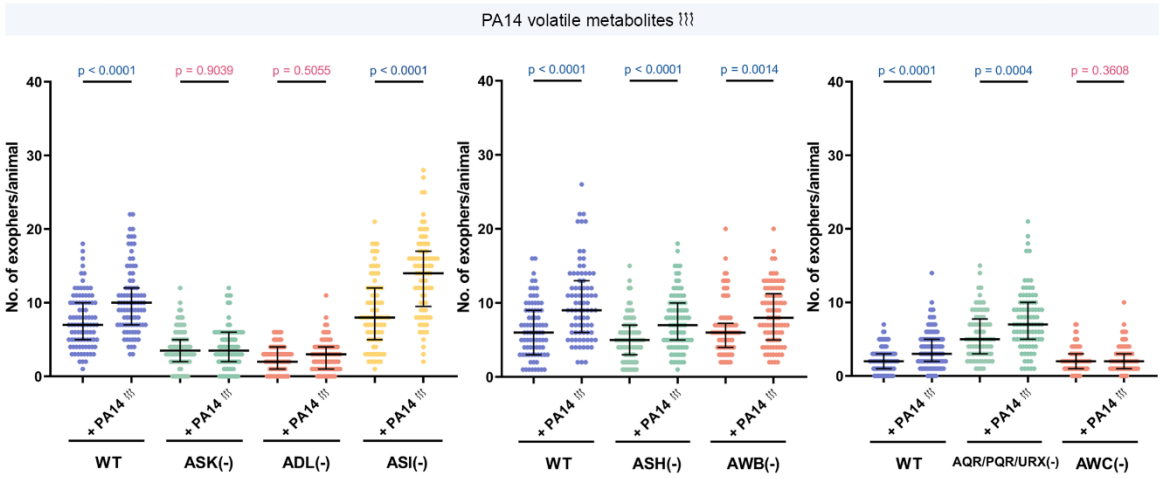

b

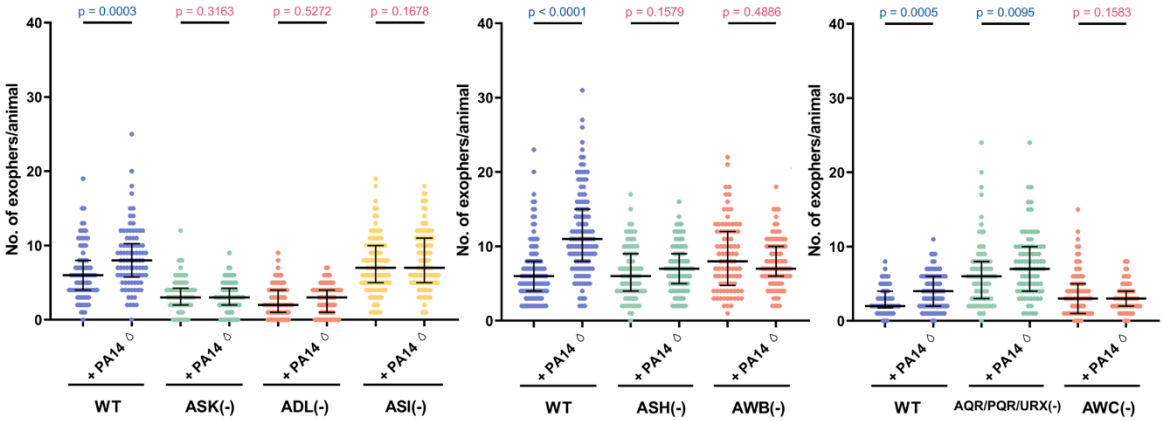

c

	PA14 volatile metabolites	PA14 supernatant
ASK(-)	p = 0.9039	p = 0.3163
ADL(-)	p = 0.5055	p = 0.5272
ASI(-)	p < 0.0001	p = 0.1678
AQR/PQR/ URX(-)	p = 0.0004	p = 0.0095
AWC(-)	p = 0.3608	p = 0.1583
AWB(-)	p = 0.0014	p = 0.4886
ASH(-)	p < 0.0001	p = 0.1579

729

730

Figure 4. Chemosensory neurons regulate exopher production in response to pathogen metabolite exposure.

a Exopher production upon exposure to PA14 volatile metabolites is dependent on ASK, ADL, and AWC neurons (n = 80-110 worms, N = 3-4 independent experiments). The data are presented in three separate graphs because three different exopher reporter lines, each exhibiting varying levels of basal exopher production, were used. The usage of different exopher reporter lines was due to crossing incompatibilities with specific neuronal ablation mutants.

b Regulation of exopher production upon PA14 supernatant exposure involves multiple neurons, including ASK, ADL, ASI, AWB, AWC, and ASH (n = 90-120 worms, N = 3-4 independent experiments). The data are presented in three separate graphs because three different exopher reporter lines, each exhibiting varying levels of basal exopher production, were used. The usage of different exopher reporter lines was due to crossing incompatibilities with specific neuronal ablation mutants.

c Summary of experimental results: A table summarizing the experimental findings, including p-values. Created with BioRender.com.

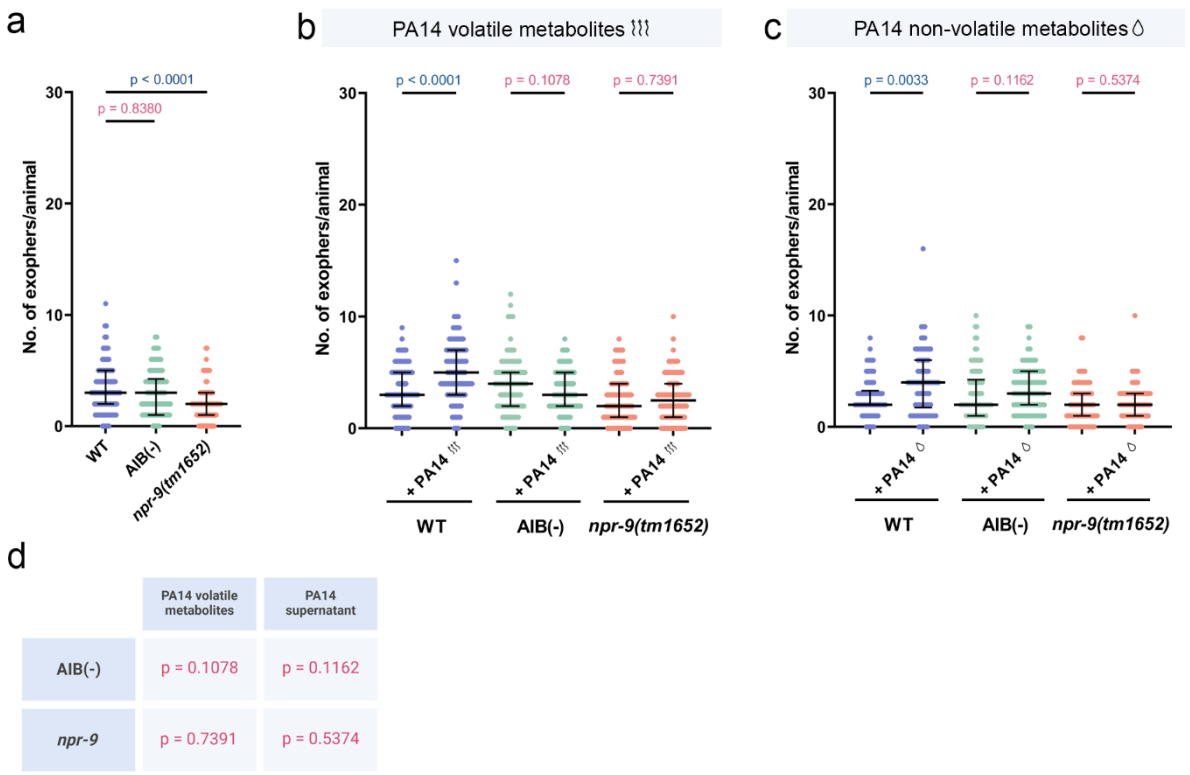

	PA14 volatile metabolites	PA14 supernatant
AIB(-)	p = 0.1078	p = 0.1162
npr-9	p = 0.7391	p = 0.5374

Figure 5. AIB interneuron and NPR-9 receptor integrate sensory responses to mediate exopher production.

a Exopher production in strains lacking the AIB interneuron or NPR-9 receptor is comparable to that in wild-type worms (n = 90 worms, N = 3 independent experiments).

b - c AIB interneuron and AIB-specific NPR-9 receptor are required for exopher production triggered by pathogen (b) volatile and (c) non-volatile metabolites (n = 88-91 worms, N = 3 independent experiments).

d Summary of experimental results: A table summarizing the experimental findings, including p-values. Created with BioRender.com.

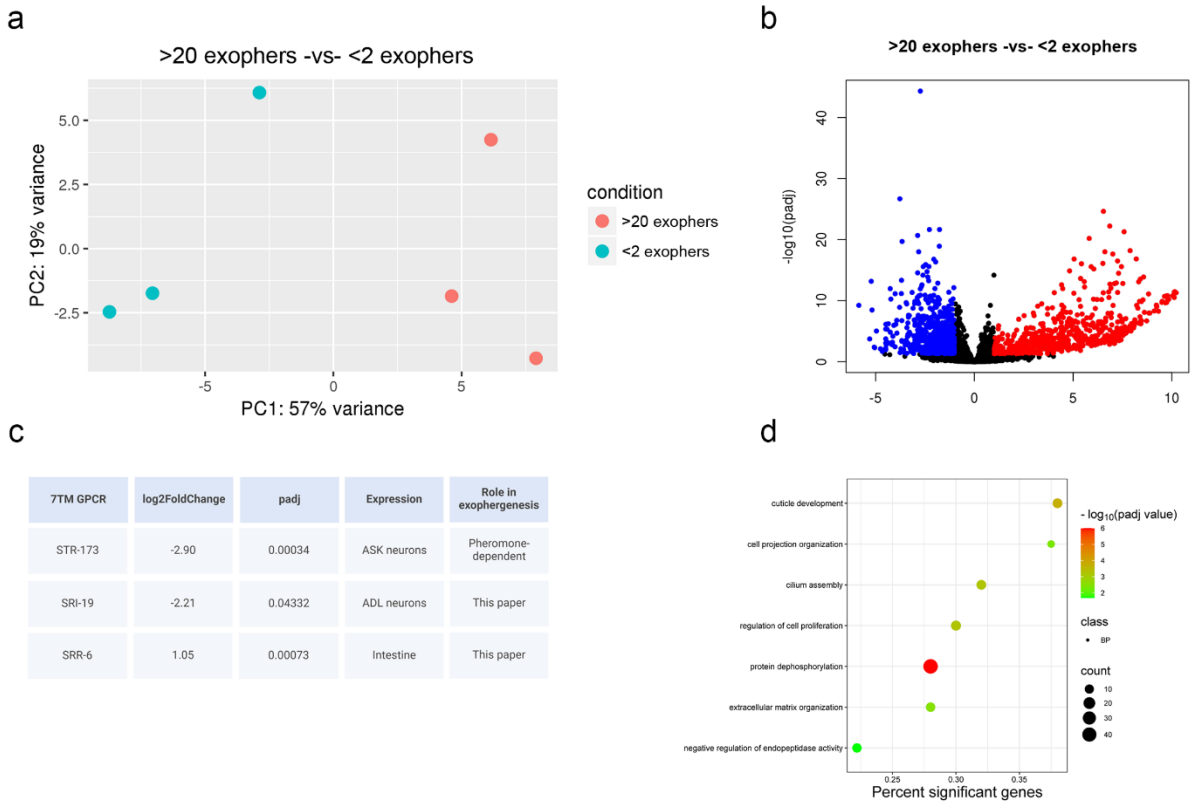

7TM GPCR	log2FoldChange	padj	Expression	Role in exophergenesis
STR-173	-2.90	0.00034	ASK neurons	Pheromone-dependent
SRI-19	-2.21	0.04332	ADL neurons	This paper
SRR-6	1.05	0.00073	Intestine	This paper

Figure 6. Comparative transcriptomic analysis of worms producing many and few exophers per individual.

a Principal component analysis (PCA) comparing worms with high exopher production (>20 exophers) and low exopher production (<2 exophers).

b Volcano plot showing differential gene expression between worms producing many exophers (>20 exophers) and few exophers (<2 exophers).

c Table listing 7TM GPCR transcripts with significant changes in expression levels.

d Gene Ontology (GO) term analysis plot based on the transcriptome results.

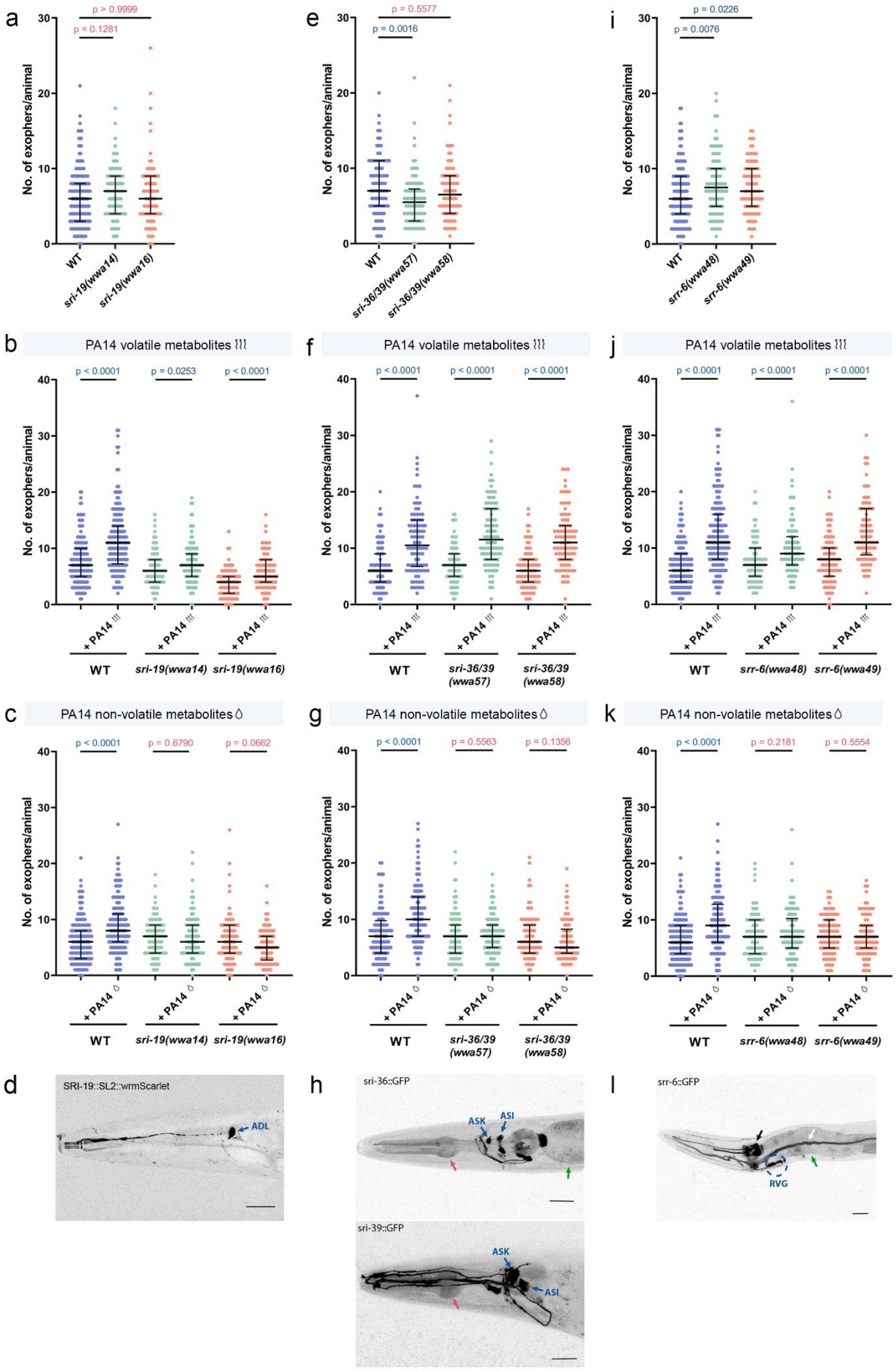
a
p > 0.9999
p = 0.1281
No. of exophers/animal
WT
sri-19(wwa14)
sri-19(wwa16)
e
p = 0.5577
p = 0.0016
sri-36/39(wwa57)
sri-36/39(wwa58)
i
p = 0.0226
p = 0.0076
srr-6(wwa48)
srr-6(wwa49)
b
PA14 volatile metabolites
p < 0.0001
p = 0.0253
p < 0.0001
+ PA14
f
p < 0.0001
p < 0.0001
p < 0.0001
sri-36/39 (wwa57)
sri-36/39 (wwa58)
j
p < 0.0001
p < 0.0001
p < 0.0001
c
PA14 non-volatile metabolites
p < 0.0001
p = 0.6790
p = 0.0662
g
p < 0.0001
p = 0.5563
p = 0.1356
k
p < 0.0001
p = 0.2181
p = 0.5554
d
SRI-19::SL2::wrmScarlet
ADL
h
sri-36::GFP
ASK
ASI
sri-39::GFP
ASK
ASI
l
srr-6::GFP
RVG

769

Figure 7. Exopher production induced by PA14 non-volatile metabolites is regulated by multiple GPCRs.

a Exopher production in worms lacking the SRI-19 receptor is comparable to that in wild-type worms (n = 90-180, N = 3-6 independent experiments).

b Increased exopher production after exposure to PA14 volatile metabolites does not depend on SRI-19 receptor (n = 90-180, N = 3-6 independent experiments).

c The SRI-19 receptor is required for exopher production induced by PA14 non-volatile metabolites (n = 90-180, N = 3-6 independent experiments).

d The *sri-19* gene encoding 7TM receptor is expressed in ADL neurons, based on position and scRNAseq data[53], consistent with observations in at least 20 animals from three replicates.

e Exopher production in worms lacking the SRI-36 and SRI-39 receptors is comparable to that in wild-type worms (n = 90, N = 3 independent experiments).

f Increased exopher production after exposure to PA14 volatile metabolites does not depend on SRI-36 and SRI-39 receptors (n = 90, N = 3 independent experiments).

g The SRI-36 and SRI-39 receptors are required for exopher production induced by PA14 non-volatile metabolites (n = 90-120, N = 3-4 independent experiments).

h The *sri-36* and *sri-39* genes encoding 7TM receptors are expressed in neurons (including ASK# and ASI#) and the alimentary tract (red arrow – pharynx, green arrow – intestine), consistent with observations in at least 20 animals from three replicates. #based on position and Vidal et al.[43].

i Basal exopher levels in *srr-6* mutants is increased compared to wild-type worms (n = 90-180, N = 3-6 independent experiments).

j Increased exopher production after exposure to PA14 volatile metabolites does not depend on SRR-6 receptor (n = 90-180, N = 3-6 independent experiments).

k The SRR-6 receptor is required for exopher production induced by PA14 non-volatile metabolites (n = 90-180, N = 3-6 independent experiments).

l The *srr-6* gene encoding 7TM receptor is expressed in neurons of the retrovesicular ganglion (encircled), pharynx neurons (black arrow), alimentary tract (green arrow – intestine), and excretory system (white arrow), consistent with observations in at least 20 animals from three replicates.

Data are presented as median with interquartile range; not significant p values ($p > 0.05$) are in pink colour, significant p values ($p < 0.05$) are in blue colour; Kruskal-Wallis test with Dunn's multiple comparisons test (a, e, i) two-tailed Mann–Whitney test (b, c, f, g, j, k). Scale bars are 20 μm.

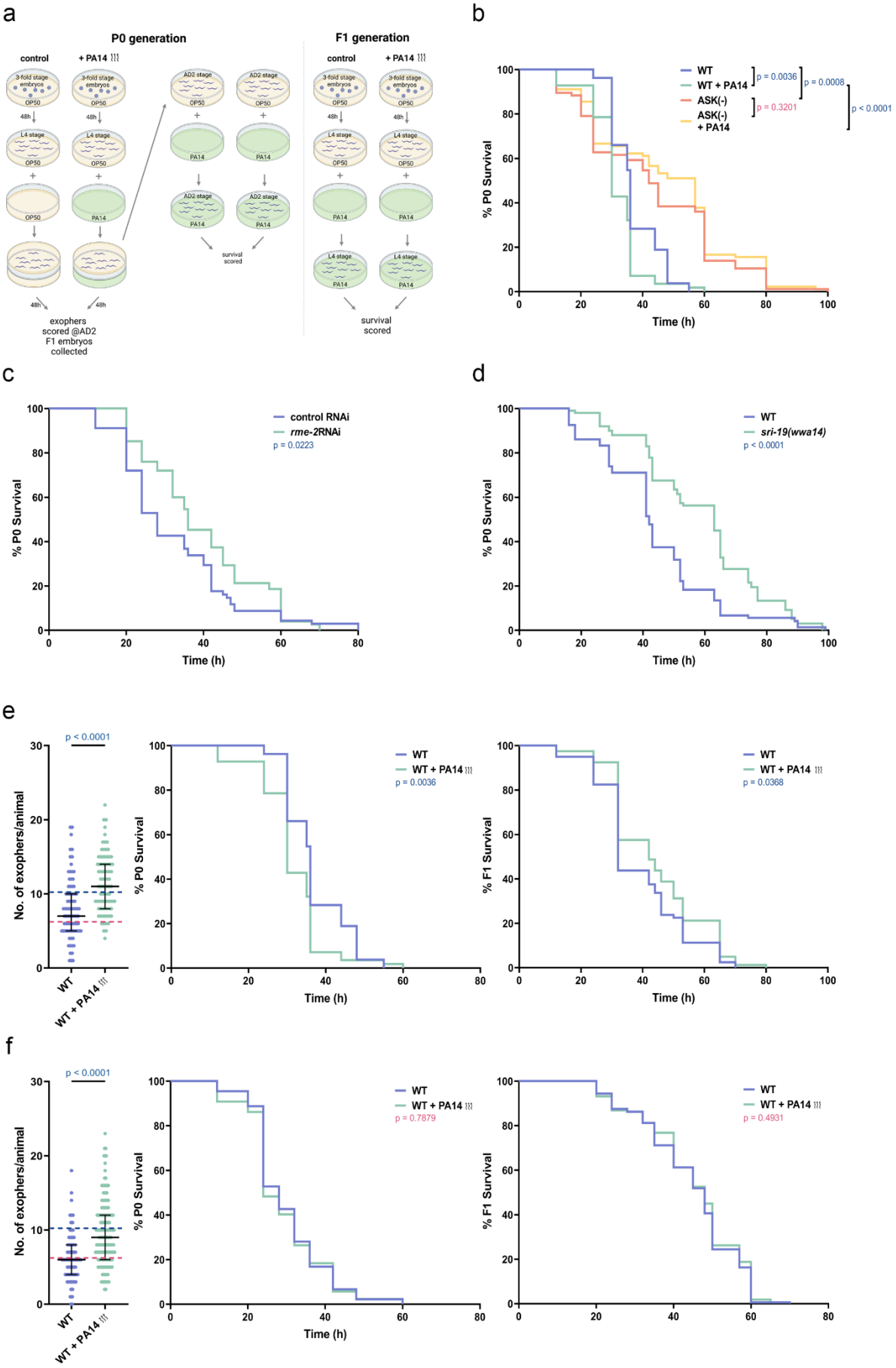
a
P0 generation
F1 generation
control
+ PA14
3-fold stage embryos
OP50
48h
L4 stage
PA14
AD2 stage
survival scored
exophers scored @AD2
F1 embryos collected
b
WT
WT + PA14
ASK(-)
ASK(-) + PA14
p = 0.0036
p = 0.0008
p = 0.3201
p < 0.0001
% P0 Survival
Time (h)
c
control RNAi
rme-2RNAi
p = 0.0223
d
WT
sri-19(wwa14)
p < 0.0001
e
p < 0.0001
No. of exophers/animal
p = 0.0036
% F1 Survival
p = 0.0368
f
p = 0.7879
p = 0.4931

804

Figure 8. Exophers levels are affecting survival rate post-infection.

a Experimental setup schematic: Age-synchronized L4-stage worms were exposed to PA14 volatile metabolites for 48 hours. After this exposure, exopher production was quantified at the AD2 stage, and embryos from the F1 generation were collected. The P0 worms were subsequently transferred to Slow Killing (SK) plates seeded with PA14, where their survival was monitored. Once the F1 worms reached the L4 stage, they were subjected to a PA14 infection assay to assess their survival. Created with BioRender.com.

b Wild-type worms exposed prior to infection to pathogen-derived volatile metabolites exhibited reduced survival compared to the control group. In contrast, worms with ablated ASK neurons, which produce low number of exophers, showed significantly improved survival, regardless of prior exposure to volatile metabolites (n = 53-90 worms, N = 3-5 independent experiments).

c Worms with *rme-2* gene knockdown, which produce low number of exophers, demonstrated enhanced survival rates upon PA14 infection (n = 68-75 worms, N = 4 independent experiments).

d The SRI-19 receptor that regulate exopher production upon exposure to PA14 non-volatile metabolites also regulates survival in response to PA14 infection (n = 102-108 worms, N = 4 independent experiments).

e F1 animals from the high exopher-producing group showed significantly longer survival after infection compared to control F1 animals, although the P0 animals had significantly shorter lifespans (n = 53-87 worms, N = 3 independent experiments).

f In contrast, there was no statistically significant difference in survival between the low exopher-producing group and the control group for either the P0 or F1 generations (n = 83-183 worms, N = 4-6 independent experiments).

Graphs (b-f) are plotted as Kaplan–Meier survival curves, not significant p values ($p > 0.05$) are in pink color, significant p values ($p < 0.05$) are in blue color.

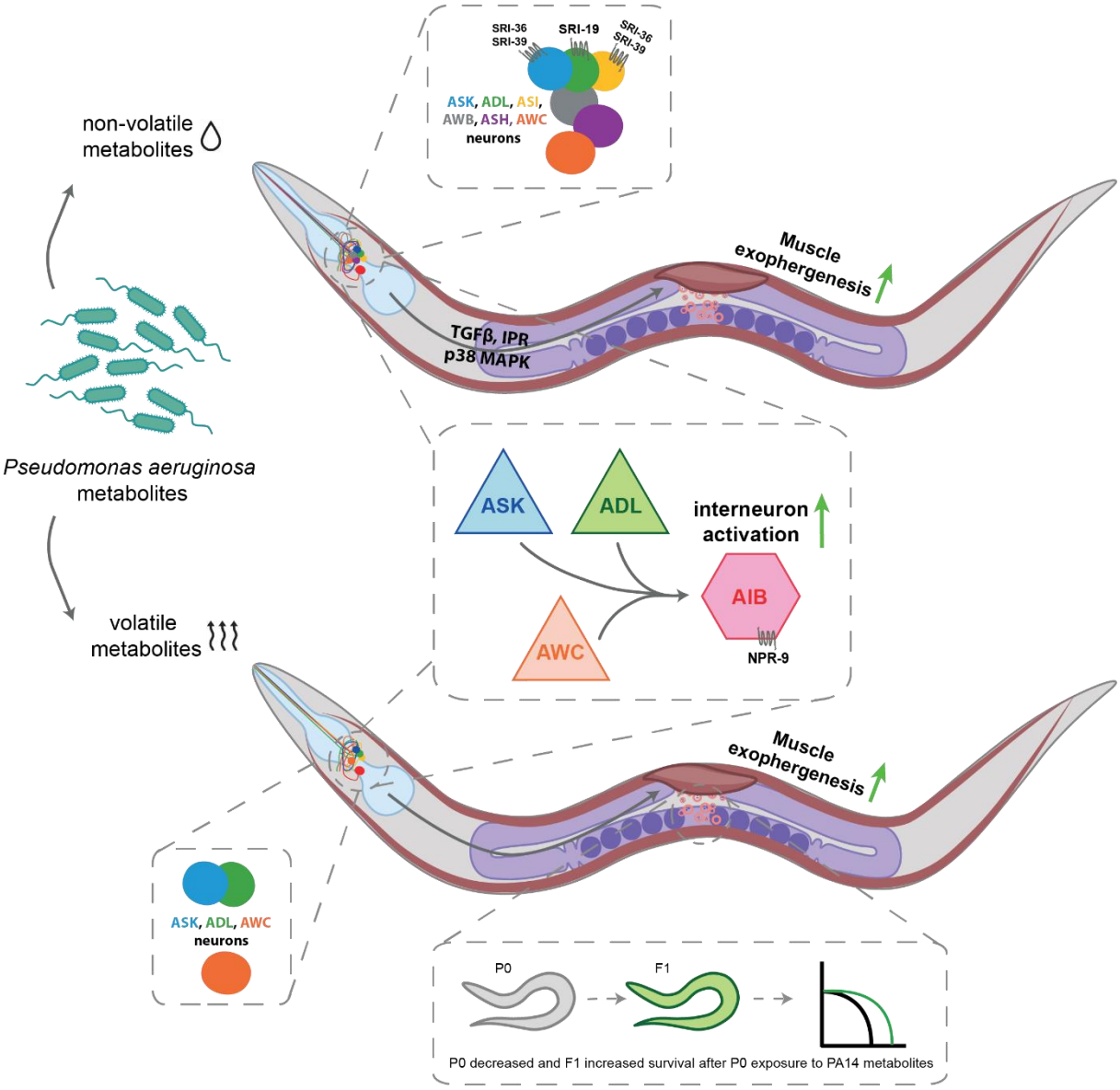

Figure 9. Model of exopher regulation from muscles by pathogen non-volatile and volatile metabolites.

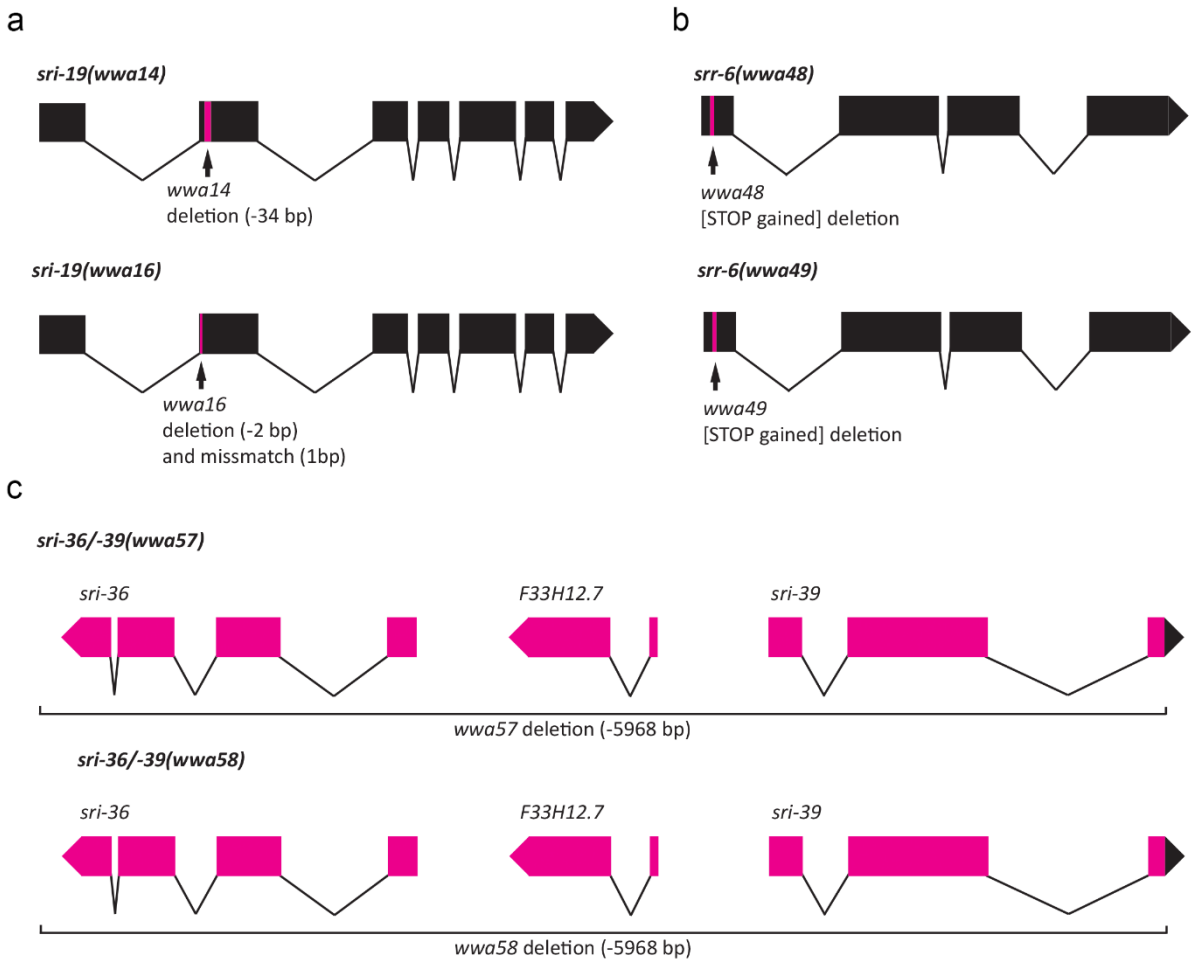

Supplementary Figure 1. Diagrams of (a) *sri-19*, (b) *srr-6*, (c) *sri-36*, and *sri-39* genomic structures and genetic lesions (marked in pink) used in the study (related to Materials and Methods).

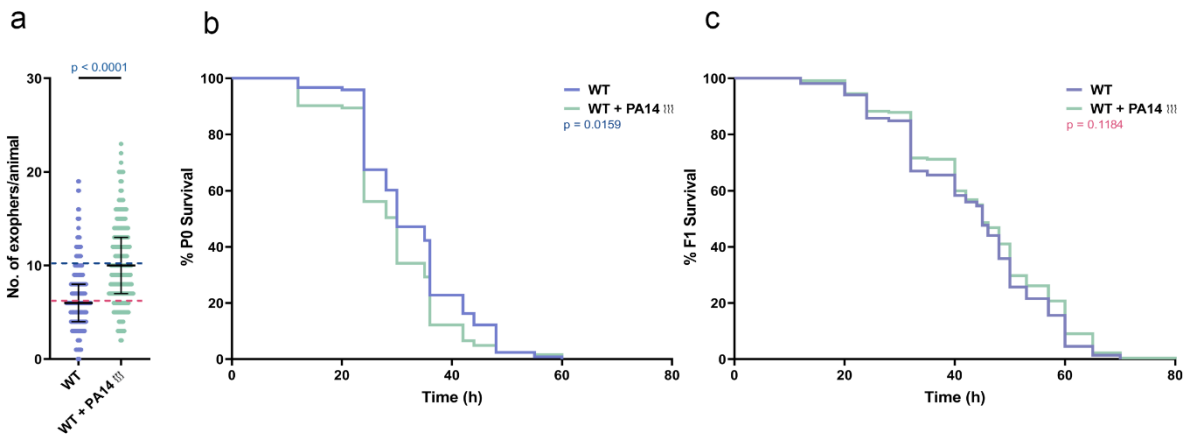

Supplementary Figure 2. Exophergenesis levels influence post-infection survival rates.

a – c Summarized data from Fig. 8e and 8f show that (a) basal exopher production did not exceed a median of 6 exophers per animal in the control group and 10 exophers per animal in the exposed group. (b) No statistically significant beneficial effect on offspring survival was observed following P0 exposure to PA14 volatile metabolites. While the P0 generation exposed to PA14 volatile metabolites showed reduced survival after infection (n = 123-233 worms, N = 6-8 independent experiments).

Graphs (b-c) are plotted as Kaplan–Meier survival curves, not significant p values ($p > 0.05$) are in pink colour, significant p values ($p < 0.05$) are in blue colour.